Journal of Mines, Metals and Fuels, *71(10): 1401-1410; 2023. DOI: 10.18311/jmmf/2023/35808*

Print ISSN : 0022-2755

Journal of Mines, Metals and Fuels

**Contents available at:** *www.informaticsjournals.com/index.php/jmmf*

# Study of Radiative Heat Transfer of Third-Grade Nanofluid Flow with Variable Viscosity in Post-Treatment Analysis of the Wire Coating Process

**Soniya Hegde[1]* and N. Srikantha[2]**

*[1]Research Scholar, Department of Mathematics, Ramaiah Institute of Technology (Affiliated to VTU), Bengaluru - 560054, Karnataka, India; soniyahegde@gmail.com*

*[2]Assistant Professor, Department of Mathematics, Ramaiah Institute of Technology (Affiliated to VTU), Bengaluru - 560054, Karnataka, India; srikantha087@gmail.com*

## Abstract

*Wire coating technology plays a pivotal role in ensuring the efficiency, safety, and sustainability of mining operations. Its contributions go beyond the surface, impacting various aspects of mining activities, from safety compliance to energy efficiency and environmental responsibility. To attain maximum efficiency in the wire/cable coating process, the foremost concern of any scientists, experts and technologists is to consider the concept of wall shear stress, heat, and mass transfer phenomenon in the interior of dyes. The fundamental requirement of the coating process is to improve the rate of heat transfer. Therefore, the purpose of the current work is to ascertain how suspended nanoparticles influence the phenomenon of heat and mass transfer rate during the post-treatment of the coating process in the presence of third-grade liquid. The Buongiorno model is employed to examine the thermophoresis and Brownian features of nano-liquid. The governing equations are formulated and simplified using suitable non-dimensional parameters. Solutions for the non-linear differential equations are obtained numerically. The outcome of various pertinent parameters on momentum, thermal, and nanoparticle concentration profiles are delineated graphically. Further, regression analysis has been carried out to understand the importance of the correlation between heat transfer rate and flow control parameters.*

**Keywords:** *Third–grade Fluid, Variable Viscosity Model, Wire Coating*

## 1.0 Introduction

The mining and minerals industry is crucial for the global economy, supplying essential raw materials to various sectors. Wire coating technology is of paramount importance within this industry, ensuring efficient, safe, and long-lasting mining operations. This article explores the diverse contributions of wire coating in mines and minerals, emphasizing its role in enhancing operational integrity and protecting the workforce and assets. Also, mining environments are often laden with corrosive substances. Wire coatings can be engineered to resist corrosion from chemicals and minerals. This resistance not only prolongs cable life but also maintains the integrity of the electrical systems, ensuring seamless operations[1–3].

The main objective of any practical application in industry is to achieve the optimal heat transfer phenomenon because the product quality and performance of the manufacturing tools are determined by the rate of heat transfer of the operating fluid[4]. Hence, several researchers are keen to explore the characteristics of heat transfer of non-Newtonian fluids which occurs in the coating of wire, wire drawing, polymer extrusion, etc. The importance of wire coating in industrial processes is traced in the eighteenth century. Extruded polymer (insulating material) is used to provide protection from the

*Author for correspondence

antagonistic environment and to increase the mechanical strength of cable or wire[5]. Numerous scientists employed Newtonian and non-Newtonian models to analyze the rheological behavior of the molten polymer in their conceptual studies[6–8]. Mitsoulis[9] investigated a complete study of the scientific literature on the flow of fluid and heat transmission in cable coatings up to 1986. The flow of polymer during the coating of wire has been modeled using a conical unit by Akter and Hashmi[10] and they have found the results for various wire speeds regarding a change in shear rate, viscosity, pressure distribution, and shear stress within the conical unit. The analytical solution is obtained by Siddique *et al.*[11] to scrutinize the coating of cable problem for third-grade liquid. In view of this, several researchers discussed the coating process of Newtonian and various non – Newtonian liquids[12–17].

Mathematicians, designers, and computer engineers have all been interested in various elements of flow analysis of non – Newtonian fluids, and therefore, the investigation of non-Newtonian fluid flows has gained prominence during the last few decades. Numerous models such as second-grade, third-grade liquids, etc. have proposed to understand the non – Newtonian characteristics of the liquids. Specifically, the third grade liquid model explains the non – Newtonian behavior like dilatant or pseudoplastic along with the normal stresses. The aforementioned facts inspired to investigate the fluid flow and thermal transmission in the process of cable coating by employing the rheological equations of the third-grade liquid. Nayak *et al.*[18] have studied the cable coating process of third-grade liquid by considering the constant and variable viscosity in the presence of the magnetic field. Several authors studied the wire coating process by implementing the third-grade liquid are mentioned in [19–26].

One of the most essential thermophysical features of fluid is its viscosity. Many researchers have examined flows with viscosity depending on temperature because of their real-world applications such as wire drawing, paper production, hot rolling, etc. With large temperature differences, the viscosity of the operating fluid becomes extremely sensitive and therefore the model which consists of viscosity as a function of temperature must be considered. If not, inaccuracy in the coefficient of the rate of heat transfer can be seen. Since attaining the most efficient heat transfer phenomenon is the subject of interest in many of the applications, the variable viscosity model plays a prominent role. Bhukta *et al.* [27]analyzed the impact of two different viscosity models namely, Reynolds and Vogel's model on the wire/cable coating process and compared the results with constant viscosity. Studies related to the effect of variable viscosity models on the process of cable coating are cited in [21,24,28].

The primary goal of the current investigation is to determine how the thermophoresis and Brownian motion parameters affect nanoparticles on the MHD third-grade fluid in a pressure-type die at the coating process in the presence of a temperature-dependent linear inverse model as the variable viscosity. Using suitable non-dimension parameters, the formulated non-linear ordinary differential equations are reduced and solved numerically. The influence of emerging parameters on velocity, temperature, and volume fractions is explored and displayed graphically. Further, to examine the importance of various parameters, a linear regression model for friction factor and rate of heat transmission is introduced.

## 2.0 Problem Formulation

Figure 1 demonstrates the schematic diagram of the flow structure of the cable/wire coating process. A cylinder based (r,ϕ,z) coordinate system is taken into consideration.

Assumptions considered for the formulation are:

- The molten polymer flow is steady and laminar
- Neglected gravitational force
- Buongiorno model with third-grade fluid is implemented

The current work concentrates on the consequences of the viscosity that varies with temperature and linear thermal radiation in the coating process.

## 3.0 Flow Geometry

For steady-state incompressible molten polymer, the extra stress matrix, momentum, temperature distribution, and volume fraction nanoparticles can be expressed as follows:

$$S = S(r),\ u = [0, 0, w(r)], T = T(r) \text{ and } C = C(r) \quad (1)$$

Where w is the velocity along z-component.

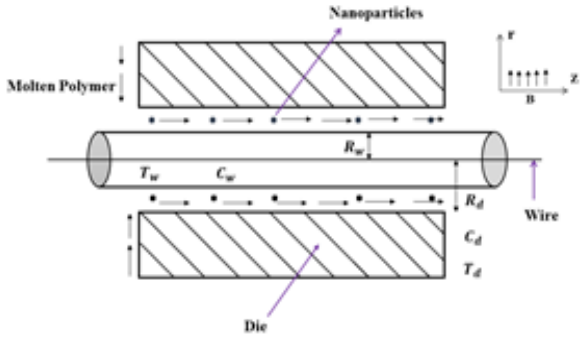



**Figure 1.** Geometry of coating process.

Following are the appropriate wiring constraints at r=$R_w$:

w=$U_w$,T=$T_w$,C=$C_w$,

Below are the boundary constraints at r=$R_d$:

w=0,T=$T_d$,C=$C_d$. (2)

S is the component of extra stress tensor and it can be defined as below for the third grade non – Newtonian liquid (24):

$$S = St_1 + St_2 + St_3 \ , \tag{3}$$

$$St_1 = \mu(T)K_1 \tag{3a}$$

$$St_2 = \alpha_1 K_2 + \alpha_2 K_2^2 \tag{3b}$$

$$St_3 = \beta_1 K_3 + \beta_2(K_1K_2 + K_2K_1) + \beta_3(trK_2)K_1 \tag{3c}$$

Where $\alpha_i's$ (i=1,2) and $\beta_j's\ (j = 1..3)$ are constants and $K_1$,$K_2$, and $K_3$ indicates the kinematic tensors, and it follows that:

$$K_1 = L_1^T + L_1 \ , \tag{4}$$

$$K_n = K_{n-1}L_1^T + L_1K_{n-1} + \frac{DK_{n-1}}{Dt}, n = 2,3 \tag{5}$$

Here, T→ Transpose of a matrix.

**Governing Equations:**

$$\nabla.\vec{u} = 0 \ , \tag{6}$$

$$\rho_f \frac{D\vec{u}}{Dt} = -\nabla p + \vec{F} + \vec{J} \times \vec{B} \tag{7}$$

$$(\rho c_p)_{nf}\left(\frac{DT}{Dt}\right) = k\nabla^2 T + \phi + (\rho c_p)_f\left(D_B\nabla T.\nabla C + \left(\frac{D_T}{T_d}\right)\nabla T.\nabla T\right) - \frac{dq_r}{dr}, \tag{8}$$

$$\frac{DC}{Dt} = D_B\nabla^2 C + \left(\frac{D_T}{T_d}\right)\nabla^2 T \tag{9}$$

Here, ρ→ density, p→ pressure, $c_p$→ specific heat at constant pressure, F→ viscous force, $\vec{J}$→ current density, $\vec{B}$→ magnetic field, k→ thermal conductivity, $D_B$→ Brownian diffusion coefficient, $q_r$→ thermal heat flux, $D_T$→ thermophoresis diffusion coefficient, ∇→ differential operator, f→ fluid, nf→ nanofluid.

From eqn. (7), $(\vec{J} \times \vec{B})$ can takes the form

$$(0, 0, -\sigma B_0^2 w(r)) \ . \tag{10}$$

Viscous dissipation function ϕ is given by,

$$\phi = \mu(T)\left(\frac{dw}{dr}\right)^2 + 2(\beta_2 + \beta_3)\left(\frac{dw}{dr}\right)^4 \tag{11}$$

The components of extra stress tensor are given by,

$$S_{rz} = \mu\frac{dw}{dr} + 2(\beta_2 + \beta_3)\left(\frac{dw}{dr}\right)^3 \tag{12}$$

$$S_{rr} = (2\alpha_1 + \alpha_2)\left(\frac{dw}{dr}\right)^2 \tag{13}$$

$$S_{zz} = \alpha_2\left(\frac{dw}{dr}\right)^2 \tag{14}$$

Using the above-mentioned equations, the conservation of momentum (7) becomes,

$$\frac{\partial p}{\partial r} = -(2\alpha_1 + \alpha_2)\frac{1}{r}\frac{d}{dr}\left\{r\left(\frac{dw}{dr}\right)^2\right\} \tag{15}$$

$$\frac{\partial p}{\partial \theta} = 0 \tag{16}$$

$$\frac{\partial p}{\partial z} = \frac{1}{r}\frac{d}{dr}\left(r\mu(T)\frac{dw}{dr}\right) + \frac{2(\beta_2 + \beta_3)}{r}\frac{d}{dr}\left\{r\left(\frac{dw}{dr}\right)^3\right\} - \sigma B_0^2 w \tag{17}$$

Equation (19) reveals that since the flow is created in a die by drag force with a uniform cross-section, the pressure gradient in the z- component is irrelevant.

$$\frac{1}{r}\frac{d}{dr}\left(r\mu(T)\frac{dw}{dr}\right) + \frac{2(\beta_2 + \beta_3)}{r}\frac{d}{dr}\left\{r\left(\frac{dw}{dr}\right)^3\right\} - \sigma B_0^2 w = 0 \tag{18}$$

The energy and nanoparticle volume fraction equations reduce to:

$$k\left(\frac{d^2}{dr^2} + \frac{1}{r}\frac{d}{dr}\right)T + \mu(T)\left(\frac{dw}{dr}\right)^2 + 2(\beta_2 + \beta_3)\left(\frac{dw}{dr}\right)^4 + (\rho c_p)_f\left(D_B\frac{\partial T}{\partial r}\frac{\partial C}{\partial r} + \frac{D_T}{T_d}\left(\frac{\partial T}{\partial r}\right)^2\right) - \frac{dq_r}{dr} = 0 \tag{19}$$

$$D_B\left(\frac{d^2}{dr^2}+\frac{1}{r}\frac{d}{dr}\right)C+\frac{D_T}{T_d}\left(\frac{d^2}{dr^2}+\frac{1}{r}\frac{d}{dr}\right)T=0 \tag{20}$$

The radiative heat flux $q_r$ is given by,

$$q_r=-\frac{4\sigma_0}{3k^*}\frac{\partial T^4}{\partial r}, \text{ and } \quad T^4=4T_w^3T-3T_w^4 \tag{21}$$

Where $\sigma_0$→ Boltzmann constant, $k^*$→ mean absorption coefficient.

## 4.0 Solution Procedure

Relevant non-dimensional variables are as follows:

$$\xi=\frac{r}{R_w},\ U=\frac{w}{U_w}$$

$$\theta=\frac{T-T_w}{T_d-T_w},\ \phi=\frac{C-C_w}{C_d-C_w},\ \gamma^*=\beta_2+\beta_3,\ \frac{R_d}{R_w}=\delta>1,$$

$$\gamma=\frac{\gamma^*U_w^2}{R_w^2\mu_0},\ Ha=\frac{\sigma B_0^2R_w^2}{\mu_0},\ Br=\frac{\mu_0U_w^2}{k(T_d-T_w)},\ Nb=D_B\frac{(\rho c_p)_f(C_d-C_w)}{k}$$

$$Nt=D_T\frac{(\rho c_p)_f(T_d-T_w)}{T_dk},\ R=\frac{16\sigma_0T_w^3}{3kk^*} \tag{22}$$

The non-dimensional variable viscosity can be expressed as [29] :

$$\mu(T)=\frac{\mu_0}{1-\frac{\theta}{\theta_r}} \tag{23}$$

Where, $\mu_0$ is the reference viscosity, $\theta_r$ signifies the non-dimensional constant and the range varies from -0.001 to -10.

Reduced Equations with appropriate boundary conditions:

$$\frac{1}{\left(1-\frac{\theta}{\theta_r}\right)}\left(\frac{d^2U}{d\xi^2}+\frac{1}{\xi}\frac{dU}{d\xi}\right)+\frac{\theta_r}{(\theta_r-\theta)^2}\frac{d\theta}{d\xi}\frac{dU}{d\xi}$$
$$+2\gamma\left(3\left(\frac{dU}{d\xi}\right)^2\left(\frac{d^2U}{d\xi^2}\right)+\frac{1}{\xi}\left(\frac{dU}{d\xi}\right)^3\right)-HaU=0 \tag{24}$$

$$(1+R)\frac{d^2\theta}{d\xi^2}+\frac{1}{\xi}\frac{d\theta}{d\xi}+\frac{Br}{\left(1-\frac{\theta}{\theta_r}\right)}\left(\frac{dU}{d\xi}\right)^2+2Br\gamma\left(\frac{dU}{d\xi}\right)^4$$
$$+Nb\left(\frac{d\phi}{d\xi}\right)\left(\frac{d\theta}{d\xi}\right)+Nt\left(\frac{d\theta}{d\xi}\right)^2=0 \tag{25}$$

$$\frac{d^2\phi}{d\xi^2}+\frac{1}{\xi}\frac{d\phi}{d\xi}+\frac{Nt}{Nb}\left(\frac{d^2\theta}{d\xi^2}+\frac{1}{\xi}\frac{d\theta}{d\xi}\right)=0 \tag{26}$$

$$U(1)=1,U(\delta)=0,\theta(1)=0,\theta(\delta)=1,\phi(1)=0,\phi(\delta)=1. \tag{27}$$

The key factors of practical interest are the local number Nur and friction factor Sf, defined as:

$$Sf=\frac{\tau_w}{\rho U_w^2},$$

$$\text{where}\quad \tau_w=\mu(T)\frac{dU}{dr}\Big|_{r=R_w} \tag{28}$$

$$Nur=\frac{R_wq_w}{k(T_d-T_w)},$$

$$\text{where}\quad q_w=-k\frac{dT}{dr}\Big|_{r=R_w}+q_r. \tag{29}$$

The dimensionless set of equations (24) – (27) are solved using MAPLE which combines Finite Difference and Richardson extrapolation procedure. Table 1 gives the comparative study with the work of Mahanthesh *et al.*[24]. The tabular values are extracted by varying magnetic parameter and omitting heat radiation, and the values are in great agreement with the earlier work.

**Table 1.** Comparison of -θ'(0) with Mahanthesh *et al.*[24]

| Ha | Mahanthesh *et al.* [24] | Present work |
|---|---|---|
| | -θ'(1) | -θ'(1) |
| 0.0 | 3.54285 | 3.54285 |
| 1.0 | 3.97423 | 3.97423 |
| 1.5 | 4.52020 | 4.52020 |

## 5.0 Result and Discussion

In this portion, the salient characteristics of a few sundry parameters, like Hartmann number (Ha), non – Newtonian parameter (γ), Brinkmann number (Br), thermophoresis (Nt), Brownian motion number (Nb), thermal radiation parameter (R), viscosity parameter ($\theta_r$) on momentum U(ξ), thermal θ(ξ), and volume

fraction ϕ(ξ) fields are performed and exhibited graphically.

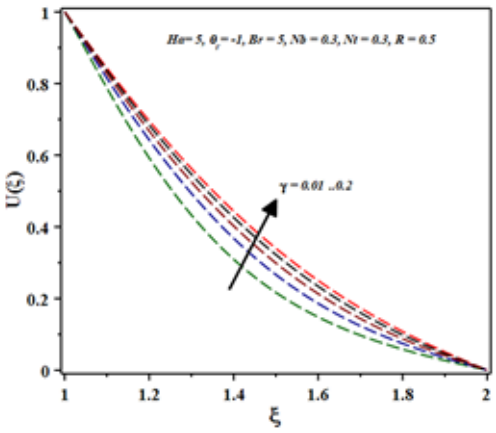



**Figure 2.** Effect of non-Newtonian parameter (γ) on U(ξ)

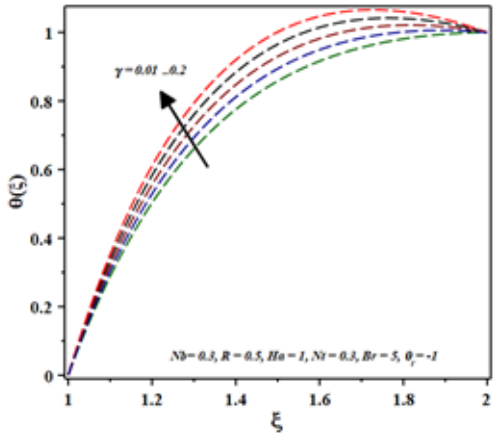



**Figure 3.** Effect of non-Newtonian parameter (γ) on θ(ξ)

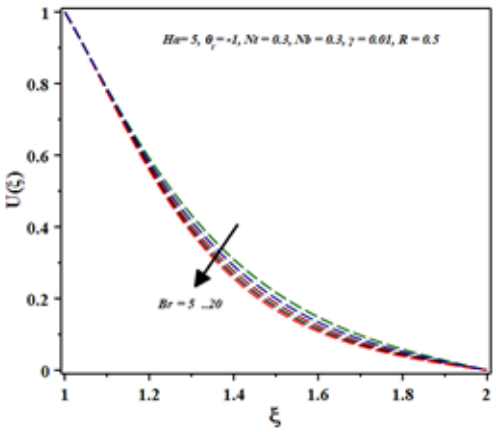



**Figure 4.** Effect of Brinkmann number (Br) on U(ξ).

Figures 2-3 delineates the consequence of third-grade factor on momentum, and temperature domains. The graph shows that the non-Newtonian behavior of the

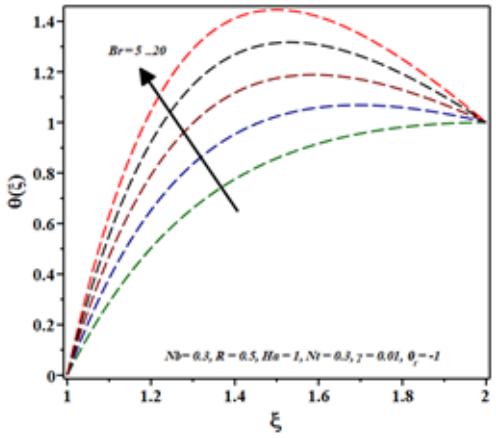



**Figure 5.** Effect of Brinkmann number (Br) on θ(ξ).

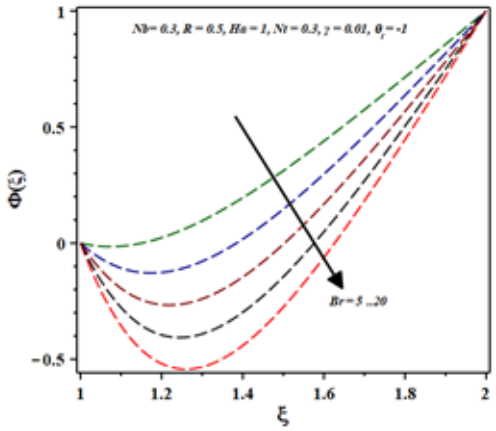



**Figure 6.** Effect of Brinkmann number (Br) on ϕ(ξ).

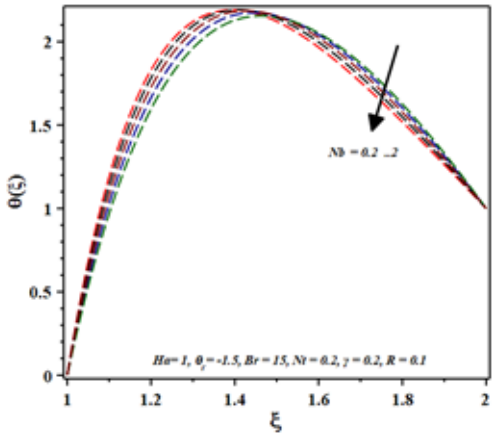



**Figure 7.** Variation of Brownian number (Nb) on θ(ξ).

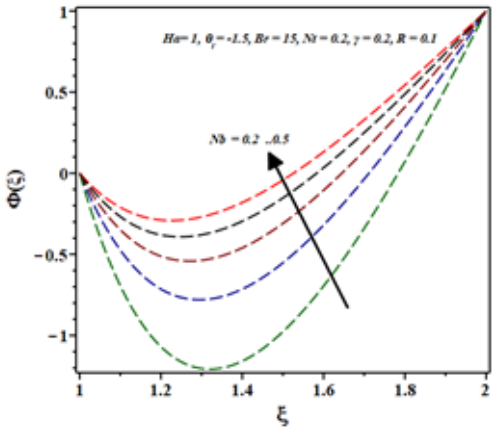



**Figure 8.** Variation of Brownian number (Nb) on ϕ(ξ).

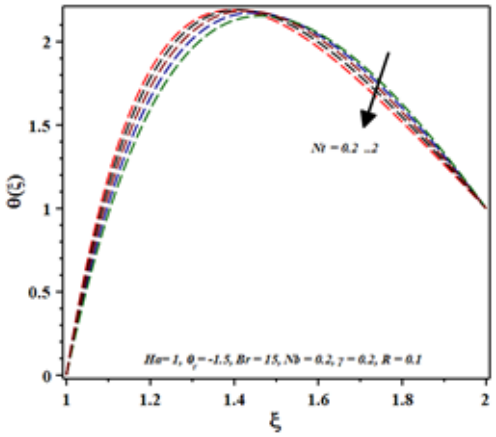



**Figure 9.** Variation of Thermophoresis parameter (Nt) on θ(ξ).

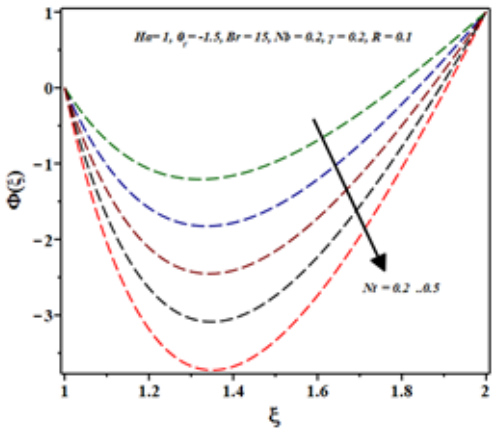



**Figure 10.** Variation of Thermophoresis parameter (Nt) on ϕ(ξ).

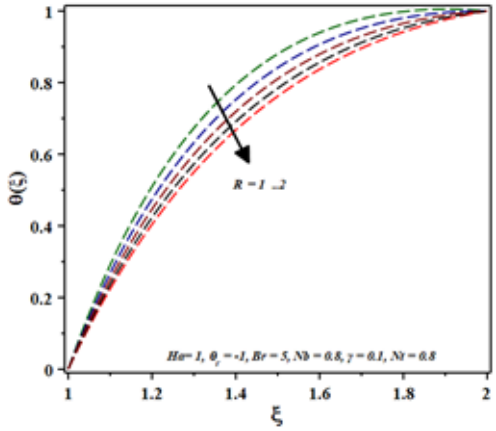



**Figure 11.** Consequence of Radiation parameter (R) on θ(ξ).

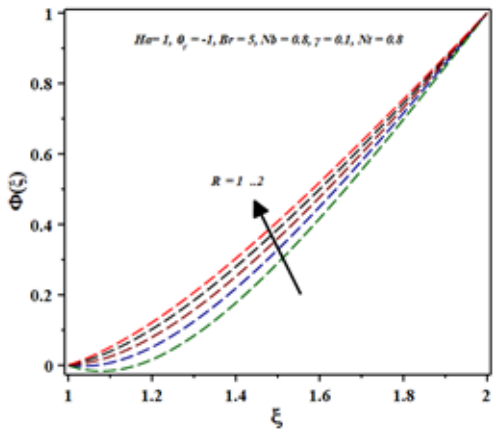



**Figure 12.** Consequence of Thermal Radiationparameter (R) on ϕ(ξ).

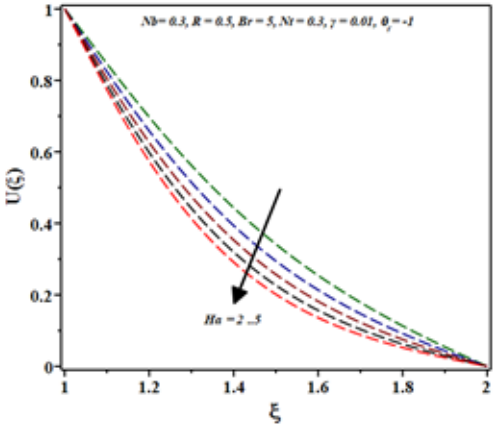



**Figure 13.** Variation of magnetic parameter (Ha) on U(ξ).

fluid enhances the velocity and heat distribution of the molten polymer near the cable surface in turn improves the coating process.

The Brinkmann number can be express as the multiple of the Eckert number and the Prandtl number. plays a major role in the cable coating process since it

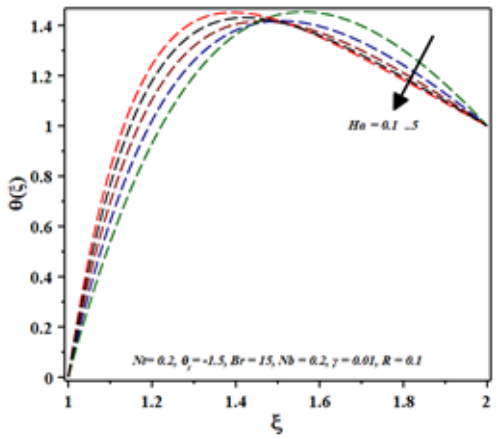



**Figure 14.** Variation of magnetic parameter Ha on θ(ξ).

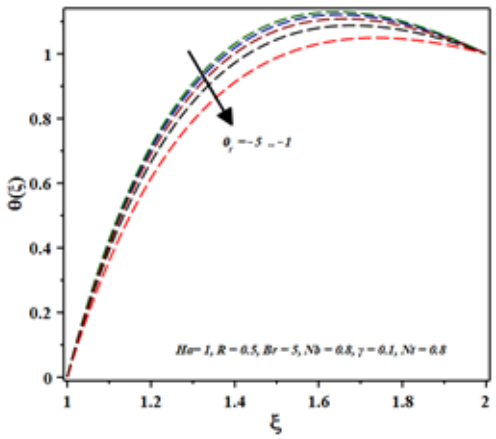



**Figure 15.** Variation of Variable Viscosity parameter $\theta_r$ on θ(ξ).

is related to conduction to the third-grade fluid from the die. Also, higher Br≫1 values, indicate a nonlinear temperature distribution behavior and it signifies a high viscous heating effect, while lower Br≪1 values lead to a linear distribution. The impact of the Brinkman number on velocity, temperature, and nanofluid volume fraction fields is portrayed in Figures 4 – 6.

As the Brinkmann number increases, the velocity, and volume fraction concentration curves diminishes. Furthermore, the temperature distribution field increases for the higher values of Br, this nature is because the viscous heating effect produces more kinetic energy. To understand how the nanoparticles affect the coating process, the Buongiorno model has been implemented. From Figures 7 – 10, one can analyze the outcome of the impacts of Brownian number and Thermophoresis on the thermal, and volume fraction concentration fields. Brownian motion exists due to the continual collision effect noticed between the nanoparticles and melted polymer substance. When nanoparticles collide, the fluid system gains more kinetic energy, resulting in a stronger thermal field and it can be noticed from Figure 7, that the temperature distribution curve rises as Nb rises when ξ varies from 1 to 1.5 and starts to decrease under the effect of various external forces. On the other hand, the volume fraction concentration field boosts up with Nb which can be visualized in Figure 8. The process of thermophoresis refers to the rapid spreading of nanoparticles caused by the temperature gradient. A higher thermophoresis number indicates a stronger thermal gradient, which raises the temperature of the nanofluid. Therefore, when 1≤ξ<1.5 as Nt increases, temperature improves. On the contrary, the volume fraction profile reduces with higher Nt values. Figures 11 – 12 conveys the outcome of the thermal radiation parameter on the temperature and volume fraction profile.

It is crystal clear that as raises, heat radiation emission increases and thereby decreases the heat transfer rate, and thus temperature field diminishes whereas volume fraction concentration raises. Figures 13–14 demonstrate the evolution of both the momentum and the temperature profile under the impact of the magnetic parameter Ha. It has been observed that higher values of magnetic parameters lead to slowing down the velocity in the fluid domain and accelerating the temperature in the interval ξ=[1,1.6]. The temperature then drops. The reason behind this is introducing a magnetic field tends to cause a drag force that restricts the flow. This drag force is termed Lorentz force. Due to this, the velocity diminishes and the thermal distribution rises in the fluid domain. The plot of the temperature field for different values of $\theta_r$ can be observed in Figure 15. Here, $\theta_r$ ranges from -5 to -1. The temperature profile decreases as $\theta_r$ increases.

## 5.1 Surface Plots

For an overview of the heat transfer rate in the model the 3-D diagrams are presented Figures 16-18. Nt, and R have a positive relationship with the Nusselt number i.e., as the range of Nt and R rises, heat transfer rate improves, while Nb,$\theta_w$, and Ha reveals the opposite trend.

Similarly, to unveil the notable impact of certain parameters on the coefficient of friction, a surface plot has been portrayed Figures 19-21. From the plot, the least

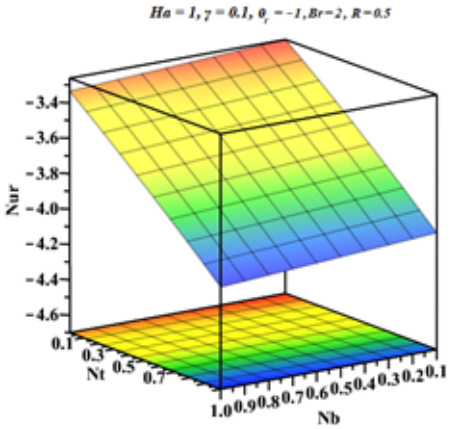



**Figure 16.** Effects of Nt,Nb on Nur.

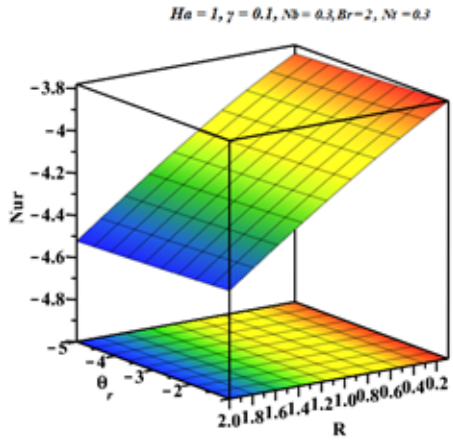



**Figure 17.** Effects of $\theta_r$,R on Nur.

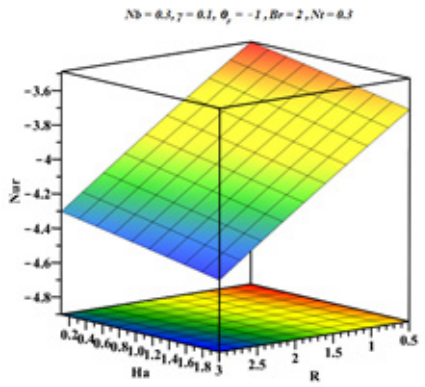



**Figure 18.** Effects of Ha,R on Nur.

Sf values are attained as Ha,Nt, and R take higher values, and in the case of Br,Nb, and $\theta_r$, Sf becomes maximum.

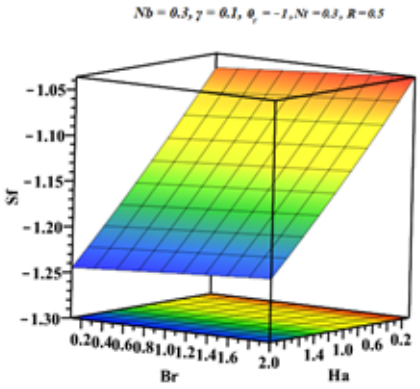



**Figure 19.** Effects of Br,Ha on Sf.

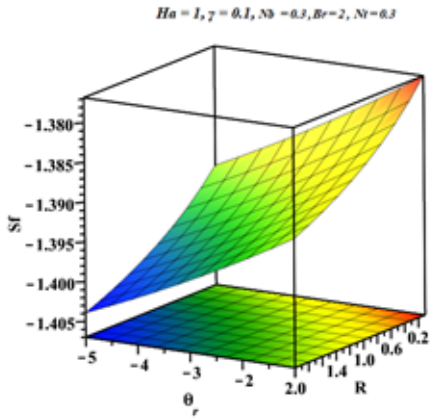



**Figure 20.** Effects of $\theta_r$,R on Sf.

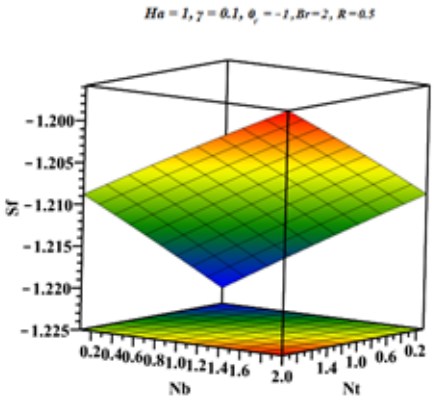



**Figure 21.** Effects Nt,Nb on Sf.

## 5.2 Regression Analysis

A linear statistical approach is considered to monitor

the performance of the parameters on the designed model. Table 2 – 3 explain the effect of some interesting parameters on and respectively with the help of 125 sets of inputs for two groups of variables.

The linear model for friction co-efficient is given by:

$$Sf = b + b_1 Br + b_2 Ha + b_3 Nb$$

Similarly, the linear model of the heat transfer rate is as follows:

$$Nur = g + g_1 Nt + g_2 R + g_3 Ha$$

**Table 2.** Linear model for Sf

| Coefficients | Estimate | Standard Error | P-value |
|---|---|---|---|
| b | -1.03725 | 0.00016 | 0.000 |
| $b_1$ | 0.01722 | 0.00029 | 0.000 |
| $b_2$ | -0.22689 | 0.00029 | 0.000 |
| $b_3$ | 0.02003 | 0.00029 | 0.0000 |

**Table 3.** Linear model for Nur

| Coefficients | Estimate | Standard Error | P-value |
|---|---|---|---|
| g | -2.24999 | 0.00186 | 0 |
| $g_1$ | -0.85933 | 0.00346 | 0 |
| $g_2$ | -0.82544 | 0.00346 | 0 |
| $g_3$ | -0.09784 | 0.00346 | 0 |

Here b is constant, $b_1$,$b_2$, and $b_3$ are the regression coefficients assessed friction factor. Further, g is constant and the coefficients of the computed regression for the heat transfer rate are $g_1$ ,$g_2$, and $g_3$.

The P-value of each coefficient describes the importance of the parameter in the model. From the table, one can clearly understand that every variable is in excellent agreement with the regression model.

## 6.0 Conclusion

In this work, we explore how the presence of nanoparticles influences the dynamics of a third-grade MHD fluid during the coating process, with a view to optimizing mining operations. The following are the notable remarks that summarise the current investigation:

- The non-Newtonian parameter enhances both the velocity and the temperature domain.
- Brinkmann number diminishes the velocity and the concentration profiles and the improves the temperature profile.
- Heat transfer rate increases with Nt, and R.
- Friction factor reduces for Ha, Nt, and R.
- Regression analysis disclose that pertinent parameters such as Ha, Nt, Nb, Br and R are favourable to attain maximum heat transfer rate.

## 7.0 References


1. Singh RP, Mallick M, Verma MK. Studies on failure behaviour of wire rope used in underground coal mines. Eng Fail Anal. 2016 Dec; 70:290–304.
2. Kumar K, Goyal D, Banwait SS. Effect of Key Parameters on Fretting Behaviour of Wire Rope: A Review. Archives of Computational Methods in Engineering. 2020 Apr 22; 27(2):549–61.
3. Xu C, Peng Y, Zhu Z, Tang W, Huang K. Influence of different mineral particles in lubricating grease on the fretting behavior between steel wires under different contact forms. Wear. 2021 May; 472–473:203700.
4. Kays W M. Convective Heat and Mass Transfer. New York: McGraw-Hill; 1966.
5. McKelvey J M. Polymer Processing. New York: Wiley; 1962.
6. Han CD, Rao D. Studies on wire coating extrusion. I. The rheology of wire coating extrusion. Polym Eng Sci. 1978 Oct; 18(13):1019–29.
7. Caswell B, Tanner RI. Wirecoating die design using finite element methods. Polym Eng Sci. 1978 Apr; 18(5):416–21.
8. Carley JF, Endo T, Krantz WB. Realistic analysis of flow in wire-coating dies. Polym Eng Sci. 1979 Dec; 19(16):1178–87.
9. Mitsoulis E. Fluid flow and heat transfer in wire coating: a review. Advances in Polymer Technology. 1986; 6:467–87.
10. Akter S, Hashmi MSJ. Analysis of polymer flow in a conical coating unit: a power law approach. Prog Org Coat. 1999 Nov; 37(1–2):15–22.
11. Siddiqui AM, Haroon T, Khan H. Wire Coating Extrusion in a Pressure-type Die in Flow of a Third Grade Fluid via Homotopy Perturbation Method. International Journal

of Nonlinear Sciences and Numerical Simulation. 2009 Jan; 10(2).
12. Mutlu I, Townsend P, Webster MF. Simulation of cable-coating viscoelastic flows with coupled and decoupled schemes. J Nonnewton Fluid Mech. 1998 Jan; 74(1–3):1–23.
13. Sajid M, Siddiqui AM, Hayat T. Wire coating analysis using MHD Oldroyd 8-constant fluid. Int J Eng Sci. 2007 Feb; 45(2–8):381–92.
14. Sajid M, Hayat T. Wire coating analysis by withdrawal from a bath of Sisko fluid. Appl Math Comput. 2008 May; 199(1):13–22.
15. Ali N, Javed MA. Effects of temperature-dependent properties on wire-coating from a bath of FENE-P fluid. Int J Heat Mass Transf. 2016 Dec; 103:401–10.
16. Basavarajappa M, Bhatta D. Heat and mass transfer of a molten polymer conveying nanoparticles in a wire coating process with temperature-dependent fluid properties: Optimization using Response surface method. International Communications in Heat and Mass Transfer. 2022 Apr; 133:105941.
17. Srikantha N, Hegde S. Numerical investigation of heat and mass transfer of the Sisko fluid in a wire-coating process with variable fluid properties. Phys Scr. 2023 Oct 1;98(10):105221.
18. Nayak MK, Dash GC, Singh LP. Steady MHD flow and heat transfer of a third grade fluid in wire coating analysis with temperature dependent viscosity. Int J Heat Mass Transf. 2014 Dec; 79:1087–95.
19. Shafieenejad I, Moallemi N, Moallemi N, Novinzadeh AB. An analytic approximation of wire coating analysis for third-grade magneto-hydrodynamic flow. Proc Inst Mech Eng C J Mech Eng Sci. 2009 Oct 1; 223(10):2273–80.
20. Nayak MK, Dash GC, Singh LP. Steady MHD flow and heat transfer of a third grade fluid in wire coating analysis with temperature dependent viscosity. Int J Heat Mass Transf. 2014 Dec; 79:1087–95.
21. Nayak M K. Wire coating analysis in mhd flow and heat transfer of a third grade fluid with variable viscosity in a porous medium with internal heat generation/absorption and joule heating. AMSE. 2016; 85(1):105–22.
22. Marinca V, Herisanu N. Approximate analytic solutions for steady MHD flow and heat transfer of a third grade fluid in wire coating process with constant viscosity. In 2017. p. 460003.
23. Khan Z, Ali Shah R, Altaf M, Islam S, Khan A. Effect of thermal radiation and MHD on non-Newtonian third grade fluid in wire coating analysis with temperature dependent viscosity. Alexandria Engineering Journal. 2018 Sep; 57(3):2101–12.
24. Mahanthesh B, Gireesha BJ, Archana M, Hayat T, Alsaedi A. Variable viscosity effects on third-grade liquid flow in post-treatment analysis of wire coating in the presence of nanoparticles. Int J Numer Methods Heat Fluid Flow. 2018 Oct 19; 28(10):2423–41.
25. Khan Z, Khan I, Ahammad NA, Basha DB, Andualem M. Effect of Nanoparticles on Wire Surface Coating Using Viscoelastic Third-Grade Fluid as a Coating Polymer inside Permeable Covering Die with Variable Viscosity and Magnetic Field. J Nanomater. 2022 May 6; 2022:1–15.
26. Zeeshan, Shaikh GM. Analysis of temperature-dependent viscosity effect on wire coating using MHD flow of incompressible third-grade nanofluid filled in cylindrical coating die. Advances in Mechanical Engineering. 2022 Apr 6; 14(4):168781322210891.
27. Bhukta D, Mishra SR, Hoque MM. Numerical simulation of heat transfer effect on Oldroyd 8-constant fluid with wire coating analysis. Engineering Science and Technology, an International Journal. 2016 Dec; 19(4):1910–8.
28. Nayak MK, Shaw S, Chamkha AJ. Radiative non linear heat transfer analysis on wire coating from a bath of third-grade fluid. Thermal Science and Engineering Progress. 2018 Mar; 5:97–106.
29. Andersson HI, Aarseth JB. Sakiadis flow with variable fluid properties revisited. Int J Eng Sci. 2007 Feb; 45(2–8):554–61.